J. COMBIN. MATH. COMBIN. COMPUT. 127b (2025) 4409--4430

Journal of Combinatorial Mathematics and Combinatorial Computing
www.combinatorialpress.com/jcmcc

Collaborative operation and supply/demand management of virtual power plant system integrating complex network theory

Jin Wang[1, ✉], Yueli Zhou[1], Shaohua Zhao[1], Zheng Weng[1], Xiaodong Zheng[1], Cong Zhang[1]

[1] *CGS POWER GENERATION(GUANGDONG)ENERGY STORAGE TECHNOLOGY CO., LTD, Guangzhou, Guangdong, 510630, China*

ABSTRACT
Virtual power plant can effectively solve the impact brought by distributed power supply access to the grid system and optimize the operational efficiency of the grid. In this paper, a virtual power plant operation system based on complex network is designed. Under the premise of taking into account the security and economy, the complex network is used to realize the automatic access of distributed energy sources and adjustable load access, put forward the topology of autonomous learning virtual power plant network, and construct the corresponding load calculation mathematical model. In addition, a day-ahead robust bidding model for multi-energy virtual power plants to participate in the peaking market is established, taking into account demand response, and the model is solved using the column and constraint generation algorithm. After the simulation experiments, a virtual power plant project containing PV, MT and wind power is analyzed as an example, and it is found that the price of electricity before 9:30 and after 16:30 is low and the purchase price is lower than the cost of VPP power generation, so in this paper, the system purchases electricity from the grid, which reduces the generation of power by generating units and reduces the cost of power generation by the system. Between 11 and 16 o'clock, the market price of electricity is very high, higher than the cost of VPP power generation, so the VPP sells electricity to the grid to gain revenue. In this paper, the operation of virtual power plant under system operation is in line with the market law, optimizing the cooperative operation and supply and demand management of virtual power plant system.

Keywords: complex network, topology, load calculation, virtual power plant, robust bidding model

1. Introduction

In order to implement the new strategy of China's energy revolution and realize the important goal of “carbon peak and carbon neutral” as soon as possible, the construction of a new type of electric power system cannot be delayed. Vigorously developing new energy sources represented by wind power and photovoltaic (PV), and gradually replacing traditional fossil energy sources with new energy sources as far as possible under the premise of ensuring the safety and reliability of the system, are the important grasps for constructing a new type of power system [1-4]. In this context, China's wind

✉ Corresponding author.
E-mail address: cnkjwangjin@126.com (J. Wang).
Received 01 January 2024; Revised 10 March 2024; Accepted 20 December 2024; Published Online 16 April 2025.
DOI: 10.61091/jcmcc127b-241

power, photovoltaic and other new energy generation continues to rise. However, with the improvement of power system intelligence, massive and diversified distributed power sources continue to emerge, and flexible and widely distributed demand-side resources are increasing, which also makes the supply pressure of the power system increasing [5-8]. However, the natural flexibility of distributed resources also brings new opportunities for the supply and demand balance and flexible regulation of new power systems [9-10]. Therefore, integrating and optimizing the flexible distributed resources and coordinating and controlling them is an important initiative to build a new type of power system.

Virtual power plant (VPP) can aggregate various types of distributed resources, such as distributed power supply, distributed energy storage, flexible adjustable loads, etc., into a flexible regulation entity through advanced communication and regulation technologies to participate in power system operation and power market transactions [11-14]. It can effectively enhance the flexible regulation capability of the power system, alleviate the problems of large peak-to-valley difference in the power grid and tight local power supply, and guarantee the safe and reliable supply of electricity [15-17]. Moreover, the virtual power plant can help improve the grid's consumption of new energy by guiding users with load regulation ability to participate in demand response, auxiliary services and other markets [18-21]. In addition, virtual power plant can guide the adjustable resources to participate in grid interaction in a market-oriented way, obtaining economic gains, reducing the cost of electricity, and improving the economic efficiency of the whole society [22-25].

In this paper, a virtual power plant operation system based on complex network is designed to construct a cooperative operation architecture of multi-energy virtual power plant. A comprehensive demand-side demand response model including cooling, heating and electricity loads is established to analyze the energy consumption characteristics of users. Considering the production, conversion and storage processes of multiple types of energy, the equipment on the energy supply side of the multi-energy virtual power plant is modeled. The average path index in complex network theory is used to evaluate the transmission energy efficiency of the distribution network containing VPPs, and the energy efficiency indexes of the two cases of entitled and un-entitled values are analyzed under the node distribution network topology, and the impacts of the interfaces between the VPPs and the distribution network and the changes in the number of VPPs in the distribution network on the energy efficiency indexes are investigated. Finally, simulation experiments and practical applications of cooperative operation and supply/demand management of virtual power plant system are carried out to test the effectiveness of the system.

2. Complex network-based virtual power plant operating system

2.1. Virtual power plant system architecture

The virtual power plant system is mainly divided into three layers of structure, respectively, the virtual power plant station control layer, process layer and resource layer, the structure is shown in Figure 1.

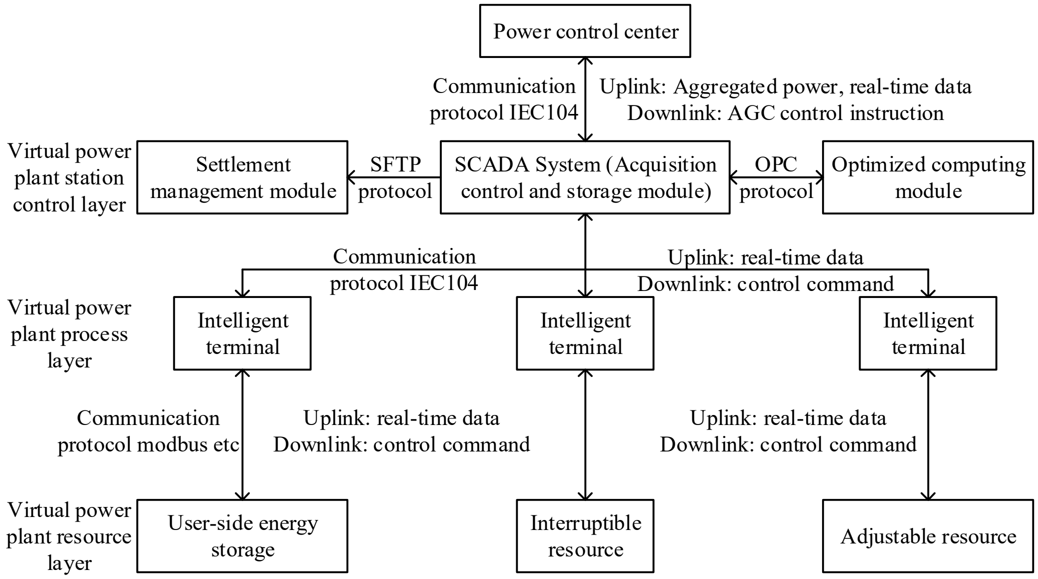

Fig. 1. Virtual power plant system structure

The process of realizing the virtual power plant application function is divided into two directions on the vertical axis: upstream and downstream.

Uplink application process: It mainly completes the process of "aggregation" of user-side energy storage, interruptible and adjustable distributed resources, collects the power and state variable information of each user resource through intelligent terminals, predicts the power of each user resource, and then evaluates the adjustable capacity of each user resource, and the adjustable power of all resources will be aggregated into a total adjustable capacity through optimization calculation. The adjustable power of all resources will be aggregated into a total adjustable capacity through optimization calculation, and the capacity and related information will be reported to the power dispatch.

Downstream application process: It mainly completes the process of "depolymerization" of distributed resources, sends out the power plan and real-time adjustment of power demand to the station control layer of the virtual power plant, which carries out optimization calculation and command decomposition, and sends them to the intelligent terminals connected to each distributed user resource. Each intelligent terminal receives the allocated power information and completes the control of the user resource equipment.

The realization of the application functions of the virtual power plant to participate in demand-side response, peak-frequency regulation and power balance requires the coordination and cooperation of each logical layer in its application functions, and the main application functions realized by each logical layer are as follows.

1) Virtual power plant resource layer. Virtual power plant user resources for the system can be accessed distributed power generation, user-side energy storage, various types of interruptible, adjustable load resources, the most typical types include distributed combustion turbines, distributed photovoltaic, user-side energy storage, charging and switching stations, building air conditioning systems, etc., these resources need to have a certain degree of flexibility and controllability, in the event of not affecting the production and operation of the electric power system according to the properties of the regulation can be divided into the resources used for frequency control Resources for peaking, such as energy storage, combustion engines, charging and switching stations, and resources for peaking, such as building air conditioners, compressors and various types of interruptible loads. Each user resource is modeled within the virtual power plant system and participates in the optimal scheduling calculations and the execution of aggregation and deaggregation algorithms, thus interacting with the grid to achieve the goals of frequency and peak regulation.

2) Virtual power plant process layer. It is mainly composed of intelligent terminals, including protocol conversion interface, miniature longitudinal encryption and communication module, which are installed in the data acquisition, communication and control equipment cabinets at the user's resource site, and its main function is to collect and measure the real-time operation data of the resources and remotely transmit them to the station control layer of the virtual power plant for optimization scheduling and computation through communication. At the same time, the intelligent terminal receives control commands issued by the virtual power plant station control layer to realize local regulation and control of resources.
3) Virtual power plant station control layer. Uplink communicates with the power control center to receive AGC commands for frequency and peak regulation issued by the dispatch, and downlinks data communication with the intelligent terminal to obtain measurement data of the connected user resources and the establishment and operation of the user resource model, and realizes optimization calculations for resource flexibility prediction, aggregation and de-aggregation based on the collected data, and sends out the optimization results of the automatic power control (APC) commands to the intelligent terminal equipment. The APC commands are sent to the intelligent terminal equipment.

2.2. Basic Concepts of Complex Networks

Many concepts and methods have been proposed to characterize the statistical properties of complex networks. For example, some basic concepts have been defined to characterize the statistical properties of network structures, such as Fig. G, average path length L, clustering coefficients C_i, and degree distributions P_k. This subsection focuses on the introduction of these basic concepts [26].

A concrete network can be abstracted as a graph $G=(V,E)$ consisting of a point set V and an edge set E. G provides a unified approach to the representation of various real networks. Depending on the directionality and the presence or absence of weighting of edges in the edge set E, one classifies graphs into four different types: directed weighted and directed unweighted graphs, undirected weighted graphs, and undirected unweighted graphs. An undirected edge (i,j) means that there is a bi-directional edge from i to j, i.e., there must be a $(i,j)=(j,i)$: while a directed edge (i,j) means that there is a unidirectional edge with point i as the starting point point pointing to the end point j, and thus in a directed graph $(i,j)\neq(j,i)$. Unweighted edge is to regard all the connected edges in the network as undifferentiated edges, and it is customary to define the weight value of all the edges as 1. Weighted edges are the edges between any two points which are assigned corresponding weight values according to the actual situation, so as to express certain meanings, for example, the weighted value of the edges in the power grid can be expressed as the transmission capacity between two points.

One usually defines the distance between two nodes i and j in a network in terms of the number of edges on the shortest path connecting the two nodes d_y and the average path length L in terms of the average of the shortest paths of all nodes in the network to each other, which is mathematically described as:

$$L=\frac{1}{\frac{1}{2}N(N-1)}\sum_{i\geq j}d_{ij} \tag{1}$$

where N is the number of nodes in the network.

In our network of friendships, two of our friends may also be friends with each other, and we make such properties the clustering properties of the network. Assuming that node i has k_i edges connected to other nodes in a network with at most one connected edge between any two nodes, we say that node i has k_i neighbors. Obviously, these k_i neighbors of node i may have at most $k_i(k_i-1)/2$ edges between them. Assuming that there are actually E_i connected edges between these

k_i neighbors, the clustering coefficient C of node i, which is used to measure the closeness between the nodes of the network, can be defined as:

$$C_i = \frac{E_i}{(k_i(k_i - 1))/2} \tag{2}$$

Then, the clustering coefficient C of the whole network is the average of the clustering coefficients C_i of all nodes in the network:

$$C = \frac{1}{N}\sum_{i=1}^{N} C_i \tag{3}$$

Thus, the larger the clustering coefficient of a network, the more connected the nodes within this network are.

The degree of a node i refers to the sum of the number of edges of other nodes that are connected to this node, usually denoted by k_i. We call the average of the degrees of all nodes in the network the average degree of the network $<k>$.

Another way to represent the degree distribution is the cumulative degree distribution function, which refers to the probability distribution of the nodes in the network whose degree values are not less than k.

$$P_k = \sum_{k'=k}^{\infty} P(k') \tag{4}$$

According to some properties of actual networks, after years of efforts by scientists, some classical complex network models have been discovered, such as regular networks, stochastic networks, small-world networks, scale-free networks, and association structure network models.

2.3. Virtual Power Plant Network Topology

2.3.1. Grid topology considering distributed energy access. The traditional power grid network model, which is generally established through the power company's power grid GIS model, establishes a topology based on the actual field network and displays it on the power grid GIS map. The main nodes of the network topology are substations, lines, transformers, customer meters, and other grid equipment resources [27]. The complexity of the grid is the sum of all nodes in the grid topology, which serves as the main parameter for the analysis of user electricity demand. The formula for its complexity can be defined as:

$$\text{Traditional grid complexity} = \sum(\text{Power supply equipment} + \text{Line length}) \tag{5}$$

This topological network is characterized by the distinction between the assets of the power supply company and the assets of the customer; the topological network of the power supply company does not contain the content of the customer's assets, and the scope of responsibility is distinguished while the nature of the assets is distinguished.

The establishment of virtual power plants does not require the construction of network equipment nodes corresponding to actual on-site grid equipment, but rather focuses on the logical relationship of each major grid equipment. Based on the distributed energy generation and Internet access characteristics of the virtual power plant, it is necessary to form the topology of the virtual power plant by adding the generation characteristics and adjustable loads on the basis of the traditional grid topology. Therefore, the virtual power plant grid complexity is the sum of all grid devices in the virtual power plant topology, and on the basis of the traditional grid complexity, the power generation devices and adjustable load devices are added, and its complexity can be defined by the formula:

$$\text{Virtual power plant network complexity} = \sum \begin{pmatrix} \text{Power supply equipment} + \text{Line length} \\ +\text{Power generation equipment} + \text{Adjustable load device} \end{pmatrix} \tag{6}$$

The virtual power plant established in this way, the power grid topology greatly exceeds the original power grid model in complexity, and the distributed power grid equipment and adjustable load equipment are changing at any time, becoming an unstable factor, and it is necessary to establish a new load calculation and prediction model to ensure the load regulation capacity of the power grid, and the ultimate purpose is to adjust the output of distributed energy equipment through the calculation of the topology in the case of excessive and small power load, and can control the influence range to the greatest extent by taking into account the adjustable load.

2.3.2. Grid load calculation. The guarantee of grid security and economy is to match the stable supply of grid loads with the demand of consumers' electricity loads. Accurate prediction calculation is the core content to ensure the stability and economy of the power grid, the original power grid is relatively simple because of the single power supply, considering the power calculation of distributed energy resources, need to combine the factors including weather, season, installed capacity, etc., and then add the adjustable load, but also need to combine with the production characteristics of the enterprise for prediction, taking into account the more factors and relatively complex, based on which, we categorize the calculation of Based on this, we categorize the calculations:

The load of the original grid is defined as P_s, then the maximum load is $P_{s\max}$.

The output of the distributed power supply is defined as P_d, and the maximum supply of electricity is $P_{d\max}$.

Although the maximum demand of the grid is P_m, the maximum power demand is $P_{m\max}$.

Considering the instability of the distributed power supply, the safe reserved power is not calculated for the distributed power supply, and the maximum safe reserved power is set to ΔP:

$$\max(\Delta P) = P_{\max} - P_{\max} \tag{7}$$

The amount of adjustable power in the region is P_c, then the maximum amount of adjustable load is $P_{c\max}$; the interval for safe operation of the grid is:

$$\max(\Delta P) \leq P_{c\max} \tag{8}$$

From the point of view of power operation economy, only when ΔP is the minimum amount, the operation economy of the grid is maximized with full consideration of the maximum though participation of distributed power sources, thus presuming that the most economical operation state is:

$$\min(\Delta P) = P_{m\max} - (P_{d\max} - P_{s\max}) \tag{9}$$

In the actual grid operation process, although the user's demand is changing throughout the day, but the overall trend of demand is in line with the curve, which can be set as a quantitative, then the power supply can also be characterized as a fixed although, then ΔP is negatively correlated with the output of the distributed power supply P_d, thus it is presumed that, assuming that the regulated power P_e in the region is only as a backup supply for the security of the grid in the region, then we are considering the electricity security and economic conditions can be defined as:

$$\max(\Delta P) - \min(\Delta P) \leq P_{\max} \tag{10}$$

According to this presumption, the main thing that needs to be regulated at present is ΔP, the load margin required for the safe operation of the grid. The main reference for the electricity security index is $P_{c\max}$, the adjustable load in the region, and the electricity economy index is $P_{s\max}$, the output capacity of distributed power sources in the region. Therefore, with the adjustable load as the security guarantee of the grid, the distributed power source can participate in the grid power supply system to the maximum extent of its ability to achieve the goal of maximizing the economy of grid operation.

2.4. Co-operation model of virtual power plant considering supply and demand

2.4.1. Objective function. The operational objective of the multi-energy virtual power plant is to minimize the daily operating cost of the energy station on the supply side (excluding the operating cost of other equipment for the time being, except for energy storage), which is calculated by the following formula:

$$\min C_{mvpp} = \sum_{t=1}^{N_{\pi}} (C_{grid}^{t} + C_{gas}^{t} + C_{DR}^{t} + C_{ESSs}^{t} - C_{sell}^{t} - C_{f}^{t}) \tag{11}$$

Where: C_{DR}^{t} is the compensation cost of regulating the load; C_{sell}^{t} is the revenue from the sale of energy; and C_{f}^{t} is the revenue gained from participation in the peaking market [28].

The cooling and heating loads of the users can satisfy the users' demand for indoor temperature and hot water temperature. Therefore, the compensation cost of cooling and heating loads is not considered in this chapter for the time being, and only the compensation cost of regulating electric loads is considered. The formula for calculating the compensation cost of users is as follows:

$$C_{DR}^{t} = c_{tr}^{t} \left| P_{tr}^{t} \right| = c_{tr}^{t} P_{trs}^{t} \tag{12}$$

$$-P_{trs}^{t} \le P_{tr}^{t} \le P_{trs}^{t} \tag{13}$$

Where: c_{tr}^{i} is the compensation price for regulating the electric load; P_{tr}^{i} is the transferred electric load power; and P_{tn}^{l} is an auxiliary variable introduced to linearize equation (12).

The energy sales revenue of the energy station includes three types of revenues from the sale of cold energy, heat energy and electricity to customers, which are calculated as follows:

$$C_{sell}^{t} = c_{se}^{t} C_{cds}^{t} + c_{sh}^{t} H_{bds}^{t} + c_{se}^{t} P_{cload}^{t} \tag{14}$$

$$\begin{cases} C_{cds}^{t} \le C_{cdbase}^{t} \\ C_{cds}^{t} \le n_{room} C_{cload}^{t} \\ H_{bds}^{t} \le H_{hdbase}^{t} \\ H_{bds}^{t} \le H_{hbad}^{t} \end{cases} \tag{15}$$

Where: C_{cds}^{i} and H_{hd}^{i} are variables introduced to protect the interests of the user side, i.e., the user's energy cost should not increase: $C_{cdebsse}^{t}$ and H_{hdbase}^{t} are the operating baselines of the cooling and heating loads, respectively; $c_{se}^{t}, c_{sh}^{t}, c_{se}^{t}$ is the selling price of cooling, heating, and electricity within the system, respectively, which is set as a fixed price in this chapter for convenience: n_{room} is the total number of rooms that need to be cooled on the user side.

The revenue of the multi-energy virtual power plant participating in the peaking market consists of two parts: the peak shaving revenue and the valley filling revenue, and the specific expression is shown in Equation (16).

$$C_{f}^{t} = \sum_{t \in T_{p}} c_{p}^{t} P_{p}^{t} + \sum_{t \in T_{v}} c_{v}^{t} P_{v}^{t} \tag{16}$$

Where: c_p^t and c_v^t are the prices for peak shaving and valley filling, respectively; P_p^t and P_v^t are the bidding power for peak shaving and valley filling, respectively; T_p and T_v are the peak shaving and valley filling periods, respectively.

2.4.2. Constraints:

1) Peaking constraints. The bidding power of a multi-energy virtual power plant to participate in the peaking market should be no less than the minimum bidding capacity (i.e., the entry threshold of the peaking market) issued by the dispatch center. The constraints for multi-energy virtual power plants to participate in bee-cutting peaking are shown in Equation (17), and the constraints for participating in valley-filling peaking are shown in Equation (18).

$$\begin{cases} x_p^t P_{f,min}^t \le P_p^t \le x_p^t P_p^{max}, t \in T_p \\ P_p^t \le (P_{basc}^t - P_{gnid}^t), t \in T_p \end{cases} \tag{17}$$

$$\begin{cases} x_v^t P_{f,min}^t \le P_v^t \le x_v^t P_v^{max}, t \in T_v \\ P_v^t \le (P_{grid}^t - P_{bac}^t), t \in T_v \end{cases} \tag{18}$$

where: P_{base}^j is the baseline power for purchasing power from the grid; P_{fmin}^j is the minimum bidding capacity issued by the dispatch center; x_p^i and x_v^i are both binary variables that represent no participation in the peaking market when 0, and participation in the peaking market when 1, and the type of peaking is peak shaving when x_p^t is 1, and valley-filling when x_v^t is 1; and $P_p^{\max}$ and $P_v^{\max}$ are the power ceilings for peak shaving bids and valley-filling bids, respectively.

2) Other constraints. Define the power balance constraints as follows:

$$P_{cen}^t + P_{c,cha}^t + P_{cbad}^t = P_{pou}^t + P_{GT}^t + P_{grid}^t + P_{c,dis}^t \tag{19}$$

$$P_{h,cha}^t + H_{hload}^t = H_{LB}^t + H_{HP}^t + P_{h,dis}^t \tag{20}$$

$$P_{c,cha}^t + n_{room} C_{cload}^t = C_{cen}^t + C_{LB}^t + P_{c,dis}^t \tag{21}$$

2.5. Day-ahead robust bidding model and its solution algorithm

2.5.1. Two-stage robust bidding model for a few days ago. This chapter considers the range of fluctuations in the power of PV, electrical, cooling and heating loads to establish the uncertainty set as shown in Equation (22).

$$U = \begin{cases} u = \{u_{ed}^t, u_{cw}^t, u_{out}^t, u_{pv}^t\} \\ u_i^t = u_{i,0}^t + b_i^{+,t} \Delta u_i^{\max,t} - b_i^{-,t} \Delta u_i^{\max,t} \\ b_i^{+,t} + b_i^{-,t} \le 1 \\ \sum_{t=1}^{T} (b_i^{+,t} + b_i^{-,t}) \le \Gamma_i \end{cases} \tag{22}$$

Where: $u_{cd}^t, u_{cw}^t, u_{out}^t$ and u_{pv}^t are the uncertain variables of initial load power, newly injected chilled water volume, outdoor temperature, and PV output power, respectively; $u_{i,0}^t$ and $\Delta u_i^{max,i}$ are the predicted values and maximum offsets corresponding to the above uncertain variables, respectively; b_i^{+J} and b_i^{-t} are binary variables that take the value of 1 to represent the upper and lower boundaries of the corresponding uncertain variable, respectively; Γ_i is the corresponding uncertainty adjustment parameter, which indicates the number of times the uncertain variable takes on the boundary value of the fluctuation interval during the scheduling cycle.

The above uncertainty variables are introduced into the pre-deterministic optimization model of the multi-energy virtual power plant:

$$\begin{cases} P_{edu}^{t} - u_{ed}^{t} = 0 \\ V_{cwu}^{t} - u_{cw}^{t} = 0 \\ T_{outu}^{t} - u_{out}^{t} = 0 \\ P_{pvu}^{t} - u_{pv}^{t} = 0 \end{cases} \tag{23}$$

x is the binary variable of the first level optimization problem, here in the short form; u and y are the uncertain and continuous variables of the second level optimization problem, respectively, in the short form.

The specific expressions for x and y are shown below:

$$\begin{cases} x = \{x_{LB}^{t}, x_{p}^{t}, x_{v}^{t}\} \\ y = \{P_{GT}^{t}, H_{LB}^{t}, C_{LB}^{t}, H_{HP}^{t}, C_{cen}^{t}, P_{cen}^{t}, P_{elad}^{t}, P_{tr}^{t}, H_{hload}^{t}, C_{cload}^{t}, \\ P_{grid}^{t}, P_{p}^{t}, P_{v}^{t}, P_{trs}^{t}, C_{cdc}^{t}, H_{hdc}^{t}, S_{l}^{t}, P_{l,cha}^{t}, P_{l,dis}^{t}, P_{edu}^{t}, V_{cwu}^{t}, T_{outu}^{t}, P_{pvu}^{t}\} \end{cases} \tag{24}$$

Optimization problems are difficult to solve directly using existing solvers. To solve the model, this chapter utilizes the Column and Constraint Generation (C&CG) algorithm to solve it.

2.5.2. Solution algorithms. At present, there are two main algorithms for solving robust optimization models, i.e., Benders algorithm and C&CG algorithm. These two algorithms have similar solving principles, mainly as follows: first decouple the original robust optimization problem into a master problem and a subproblem, and then solve the two alternately to finally achieve convergence and obtain the optimal solution of the original robust optimization problem. Compared with the Benders algorithm, the C&CG algorithm will find the worst scenario of the optimization objective in the current situation when solving the subproblems, so as to generate the variables and constraints related to the subproblems in the master problem, which can effectively improve the convergence speed of the model.

For convenience the optimization model is rewritten in the following matrix form:

$$\begin{cases} \min_{x} \quad \max_{u \in U} \quad \min_{y} \quad c^{T} y \\ \qquad\qquad\qquad\qquad s.t. \quad Ey + Fx \ge d \quad : \lambda \\ \qquad\qquad\qquad\qquad\qquad Ky = g \quad : v \\ \qquad\qquad\qquad\qquad\qquad I_{u} y = u \quad : \pi \end{cases} \tag{25}$$

where: c is the column vector of coefficients corresponding to the objective function; E, F, K, I_{u} is the matrix of coefficients under the corresponding constraints; d and g are the column vectors of constants under the corresponding constraints; and λ, v and π are the dyadic variables corresponding to the constraints in the second level of the min problem.

1) Subproblems. Firstly, the min optimization problem in the second layer of the model (25) is transformed into the corresponding dyadic problem by using the strong dyadic theory; then this dyadic problem is merged with the max optimization problem in the second layer to obtain the subproblem shown in Eq. (26).

$$\begin{cases} \max_{u,\lambda,v,\pi}(d-Fx)^T\lambda+g^Tv+u^T\pi \\ s.t.\, E^T\lambda+K^Tv+I_u^T\pi=c \\ \lambda\geq 0; v,\pi: free \\ u\in U \end{cases} \tag{26}$$

However, substituting Eq. (22) into Eq. (26) results in a form of multiplication of a binary variable with a continuous variable $(b_i^{+,t}\pi_i^t, b_i^{-,t}\pi_i^t)$, which is more difficult to solve directly using the solver. Therefore, it needs to be linearized, resulting in a single-level subproblem:

$$\max_{z^+,z^-,b^-,b^-,b,v,v}(d-Fx^-)^T\lambda+g^Tv+(u_0)^T\pi+(\Delta u^{max})^Tz^+-(\Delta u^{max})^Tz^- \tag{27}$$

$$s.t.\begin{cases} E^T\lambda+K^Tv+I_u^T\pi=c \\ \lambda\geq 0, v,\pi; firee \\ -b^+M\leq z^+\leq b^+M \\ -b^-M\leq z^-\leq b^-M \\ \pi-(1-b^+)M\leq z^+\leq \pi+(1-b^+)M \\ \pi-(1-b^-)M\leq z^-\leq \pi+(1-b^-)M \\ b^++b^-\leq 1 \\ \sum_{t=1}^{T}(b^++b^-)\leq\Gamma \end{cases} \tag{28}$$

where: x^{j-1} is a fixed value, derived from the main problem; z^+ and z^- are introduced auxiliary variables; and M is a sufficiently large number.

From this, u^j can be found and the upper bound calculated:

$$UB^j=\min\begin{Bmatrix} UB^{j-1},(d-Fx^{j-1})^T\lambda^j+g^Tv^j+(u_0)^T\pi^j \\ +(\Delta u^{max})^T(z^+)^j-(\Delta u^{max})^T(z^-)^j \end{Bmatrix} \tag{29}$$

2) Main problem. The master problem as shown in Eq. (30) is obtained by decomposing the original problem (25).

$$\begin{cases} \min\limits_{x,\eta,y^k,k=l,\cdots,j} & \eta \\ s.t. & \eta\geq c^Ty^k \\ & Ey^k+Fx\geq d \\ & Ky^k=g \\ & I_uy^k=u^k \end{cases} \tag{30}$$

Where: $u^k(k=1,\cdots,j)$ is a fixed value and is derived from the subproblem.

From this, x^j can be derived and the lower bound calculated:

$$LB^j=\eta^j \tag{31}$$

3) Solution flow. According to the above derivation, the multi-energy virtual power plant day-ahead robust bidding model is finally decomposed into the main problem and subproblems with mixed integer linear form (MILP). In summary, the C&CG algorithm is utilized to solve the problem and the solution flow is shown in Fig. 2.

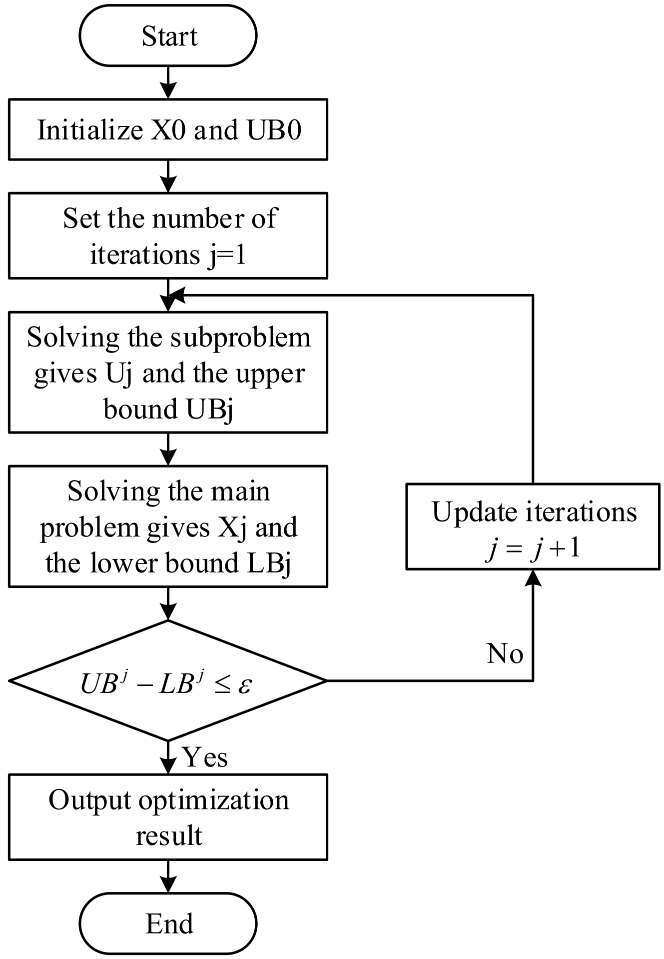

Fig. 2. Algorithm flow chart of day-ahead robust bidding model

3. System simulation and application

3.1. Characterization of virtual power plant network topology

Scale-free networks and small-world networks are typical complex network structures. Small-world networks are characterized by small average distances. The study of CPS network structure shows that the topology of physical network has scale-free network structure and the topology of information network has double star structure and mesh structure. Virtual Power Plant CPS Decentralized Architecture The control center in the virtual power plant CPS centralized architecture is represented by a node with a large node degree. The initial number of nodes in the scale-free network model constructed in this section is 30, and each time 8 new nodes are connected to the old ones, the total number of nodes in the network is 116. The small-world network is modeled as having 12 neighboring nodes per node, and the probability of reconnecting each edge in the network is 0.4 until the size of the network nodes grows to 116.

Table 1 shows the characteristic parameters of the complex network of the CPS of the virtual power plant. The average distance of the scale-free network is 1.9725 and the clustering coefficient is 0.47358. The small-world network has an average distance of 1.8137 and a clustering coefficient of 0.29496. It indicates that the nodes of the small-world network are uniformly dispersed and have smaller average distances compared to the scale-free network. In addition, the clustering coefficient of the information network in the fully decentralized architecture network of the virtual power plant CPS is larger, and the average node degree is larger, indicating that the network nodes are more closely connected to each other.

Table 1. Virtual power plant CPS characteristics parameter

Network type	Network size	Mean distance	Average node degree	Clustering coefficient
Unmarked network	116	1.9725	18.4369	0.47358
Small world network	116	1.8137	24	0.29496
Complete decentralized architecture information network	116	2.3269	35.5877	0.9056

Different coupling interdependencies between the information and physical networks of a virtual power plant can have different effects on cascade failure. In this section, a one-to-one coupling relationship between information and physical nodes is used. Existing studies indicate that nodes with large node degree are generally used to denote critical nodes. The key nodes in the information and physical networks tend to combine together as a rule. Table 2 shows the top 20 ranking of critical nodes in the virtual power plant CPS network.

Table 2. The virtual power plant CPS network key node sort

N	Small world network	Unmarked network	Complete decentralized architecture information network
1	65(31)	17(57)	86(61)
2	65(29)	22(55)	90(58)
3	28(29)	16(52)	66(58)
4	12(29)	22(52)	80(58)
5	102(29)	36(52)	89(57)
6	75(29)	27(52)	113(56)
7	41(28)	22(49)	35(55)
8	108(28)	28(46)	72(54)
9	71(28)	17(46)	78(52)
10	13(28)	14(46)	118(52)
11	64(28)	22(46)	44(52)
12	86(27)	29(42)	34(47)
13	65(26)	11(42)	102(47)
14	34(26)	20(40)	104(43)
15	65(26)	14(40)	32(42)
16	101(26)	11(40)	39(42)
17	84(26)	33(40)	60(42)
18	22(25)	30(40)	68(39)
19	45(25)	22(40)	111(37)
20	85(25)	30(40)	37(35)

3.2. Co-operative Energy Efficiency Simulation Experiments for Complex Virtual Power Plant Networks

The distribution network system used in the simulation experiment is a classical distribution network diagram, and the basic parameters of each line of this distribution network system are shown in Table 3.

Table 3. Basic parameters of 69-node distribution network

Bow node	Last point	resistance	reactance	Terminal work	No work at the end	Bow node	Last point	resistance	reactance	Terminal work	No work at the end
0	1	0.1372	0.7361	0	0	4	36	0.5002	0.1218	0	0
1	2	0.9541	0.8818	0	0	36	37	0.6301	0.3167	0	0
2	3	0.807	0.6941	0	0	37	38	0.0959	0.2173	55.1	91
3	4	0.784	0.9312	0	0	38	39	0.4338	0.1788	94.4	84
4	5	0.8175	0.7217	0	0	8	40	0.088	0.5011	0	0
5	6	0.9301	0.685	50.8	26.2	40	41	0.0722	0.4754	0	0
6	7	0.4824	0.275	76.1	60	9	42	0.7071	0.5872	0	0
7	8	0.8881	0.674	57.9	83.6	42	43	0.0515	0.4705	39	90
8	9	0.8905	0.7425	0	0	43	44	0.0911	0.0611	26.5	54.4
9	10	0.5343	0.1265	53.2	103.2	44	45	0.4966	0.606	0	0
10	11	0.0147	0.1078	0	0	45	46	0.1457	0.0139	0	0
11	12	0.5964	0.3257	0	0	46	47	0.2637	0.7052	0	0
12	13	0.469	0.9092	0	0	47	48	0.4694	0.5735	30.7	70
13	14	0.9422	0.2067	0	0	48	49	0.6207	0.8711	0	0
14	15	0.2938	0.7374	56.1	51.6	49	50	0.0245	0.1148	80.4	39.8
15	16	0.5413	0.2942	0	0	50	51	0.8823	0.5916	0	0
16	17	0.7071	0.0406	20.5	97.1	51	52	0.283	0.9251	0	0
17	18	0.4751	0.7714	50	22.6	52	53	0.056	0.4993	0	0
18	19	0.3407	0.9637	0	0	53	54	0.5762	0.9188	104.5	101.8

19	20	0.8481	0.132	32.9	28.2	11	55	0.927	0.6057	0	0
20	21	0.0677	0.5814	0	0	55	56	0.5868	0.7098	20.5	76.2
21	22	0.3847	0.1172	8.9	48.2	12	57	0.0779	0.4603	0	0
22	23	0.3544	0.8244	8.1	48.1	57	58	0.9685	0.0109	0	0
23	24	0.7457	0.4516	0	0	3	59	0.3148	0.9342	0	0
24	25	0.0269	0.3668	0	0	59	60	0.9537	0.4553	0	0
25	26	0.3125	0.9329	0	0	60	61	0.2241	0.1286	29.1	35
26	27	0.2022	0.4523	0	0	61	62	0.1367	0.5534	59.5	95
27	28	0.0619	0.4797	32.3	26	62	63	0.4614	0.4803	0	0
28	29	0.7137	0.5545	35.9	79.1	63	64	0.6227	0.1144	34.2	18
29	30	0.2515	0.6039	84.7	78	64	65	0.3782	0.0321	51.5	70.9
30	31	0.2124	0.735	0	0	65	66	0.4009	0.8732	0	0
31	32	0.0535	0.5674	0	0	66	67	0.8768	0.1548	0	0
32	33	0.8622	0.438	0	0	67	68	0.9222	0.3477	0	0
33	34	0.3753	0.0577	0	0	68	69	0.4513	0.8983	0	0
34	35	0.3939	0.5663	0	0						

1) Comparison of unauthorized and entitled networks. Table 4 shows the average path lengths and diameter sizes of the networks in the unprivileged and entitled networks. From Table 4, it can be seen that the average path of the network calculated by using the electrical distance between the network nodes instead of the shortest path when analyzing the network is shorter and the transmission energy efficiency is higher. Therefore, calculating transmission energy efficiency based on electrical distance is more realistic.

Table 4. Impact of weight on indicators

Network model	Mean path length	Diameter
No power	13.0218	24
power	1.4385	2.038

2) Comparison of results after applying the system in this paper. Since the continuous changes in the number and location of power nodes in the distribution network may adversely affect the safe and stable operation of the distribution network, the average path of the network changes when different nodes of the distribution network apply the system of this paper. Fig. 3 shows the impact of the

interface of this paper's system with the grid on the metrics when entitled and un-weighted. It can be observed that the location of the interface has a huge impact on energy efficiency irrespective of the line weights. Therefore, the location of this paper's system is particularly important when accessing the distribution network.

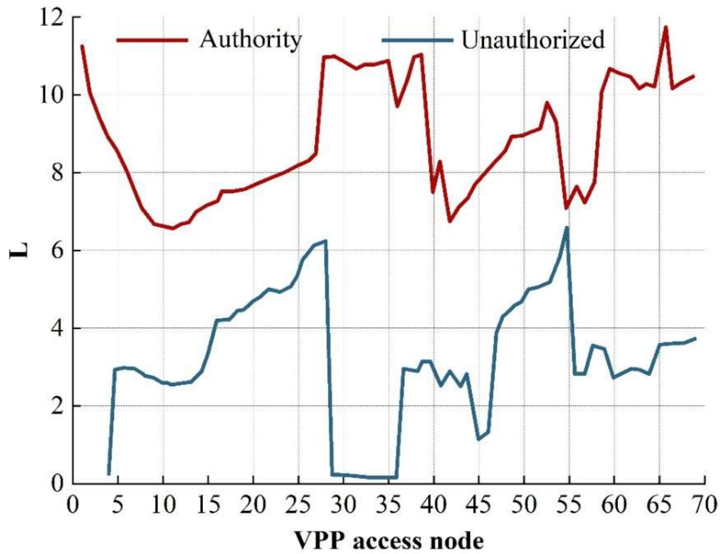

Fig. 3. The impact of interfaces on indicators

In order to better reflect the advantages of this paper's system, the microgrid and this paper's system are connected to the distribution grid at the same time to analyze the change of indicators when different nodes are accessed in both network-weighted and un-weighted scenarios. Because the energy exchange between the microgrid and the distribution network is only through a PCC interface, the variation curves of the average paths when comparing the microgrid and this paper's system accessed at different locations when the connection point is the same as 1 are shown in Fig. 4 and Fig. 5, respectively.

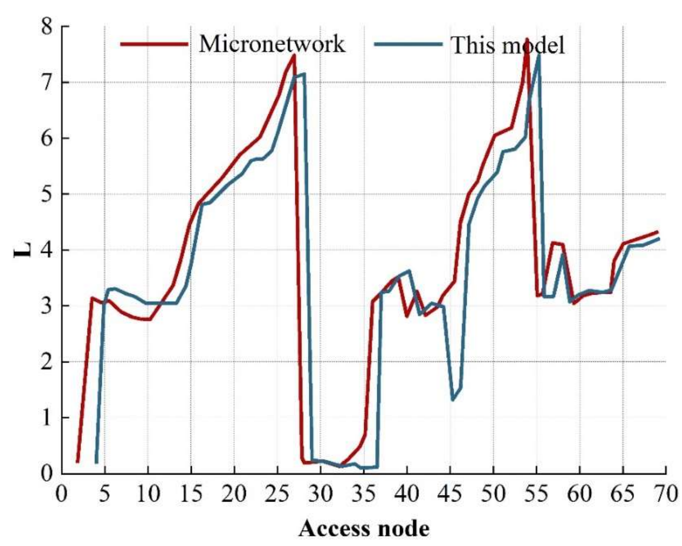

Fig. 4. Indicators of model and micro-grid access by different nodes

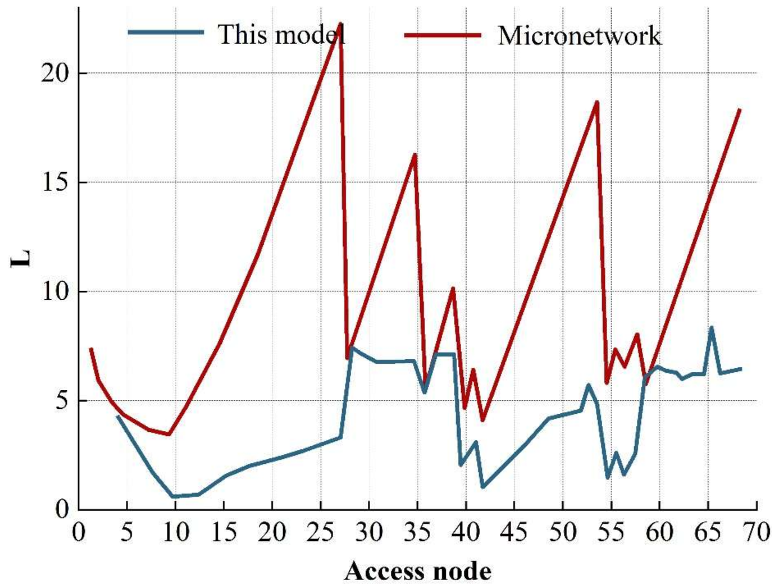

Fig. 5. Indicators of model and micro-grid access by different nodes

Therefore, it can be seen that the average path change of accessing this paper's system when the line is unweighted is smooth and smaller than the average path when the same node is accessing the microgrid, and the average path fluctuation amplitude when entitled is roughly the same, but the system of this paper's is slightly smaller compared to that of the microgrid, so that the transmission of power is smoother and more energy-efficient when accessing this paper's system in the distribution network.

3.3. Practical application of the project

3.3.1. Project data. In order to verify the feasibility and applicability of the optimized scheduling model of the virtual power plant (VPP) designed in this paper, this study conducts an application analysis for a real project condition.

This section of the VPP consists of one wind farm, one photovoltaic (PV) farm, and four gas turbines (MT), and is dispatched with the objective of minimizing operating costs.

The basic data of this project are as follows, where the electricity price is the day-ahead price, which is shown in Table 5; the upper and lower limits of wind and PV unit outputs are shown in Table 6; the MT parameters are shown in Table 7; and the wind, PV, and load forecasts are shown in Figure 6.

Table 5. Current price of electricity

Time period	Electricity price/(MWh)	Time period	Electricity price/(MWh)
1	240	13	990
2	180	14	1490
3	130	15	990
4	100	16	790
5	150	17	400
6	200	18	360
7	270	19	360
8	390	20	410
9	520	21	440
10	530	22	350
11	810	23	300
12	1000	24	230

Table 6. Wind, light unit parameters

Type	Output limit/MW	Limit/MW
Wind power unit	12	0
Photovoltaic set	16	0

Table 7. Gas turbine unit parameters

Type	Cost factor a	Cost factor b	Cost factor c	Output limit/MW	Limit/MW	Climbing power/MW
MT1	2.5	155	120	12	0	10
MT2	4	165	100	12	0	10
MT3	3.5	175	110	8	0	8
MT4	4	165	100	8	0	8

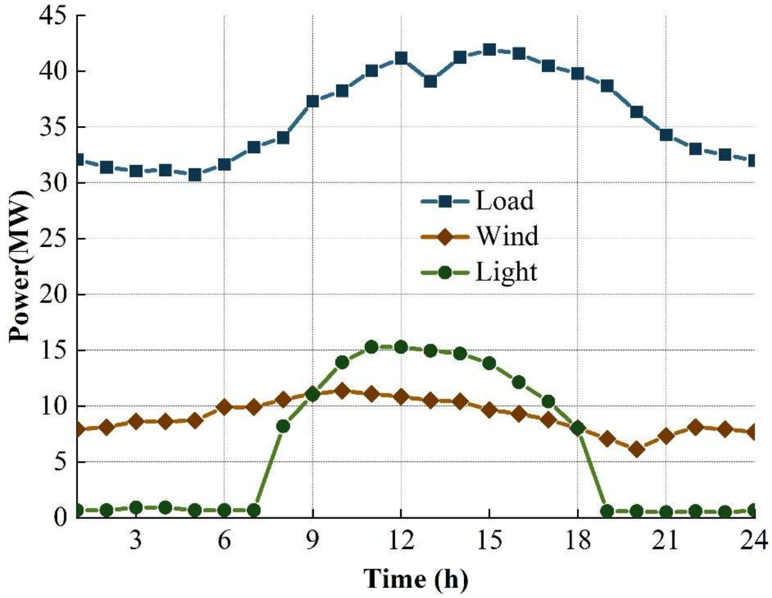

Fig. 6. Wind, light, load prediction curve

3.3.2. Experimental results. The day-ahead scheduling results of each unit of VPP are shown in Fig. 7, in which the total purchased and sold power indicates the value of VPP interacting with the power market, and the value is positive when power is purchased from the power market and negative when power is sold to the power market. From the figure, it can be seen that the sum of output and power purchase and sale of each unit is exactly equal to the total load, which indicates that the scheduling results satisfy the balance of supply and demand, and verifies the correctness of the scheduling model.

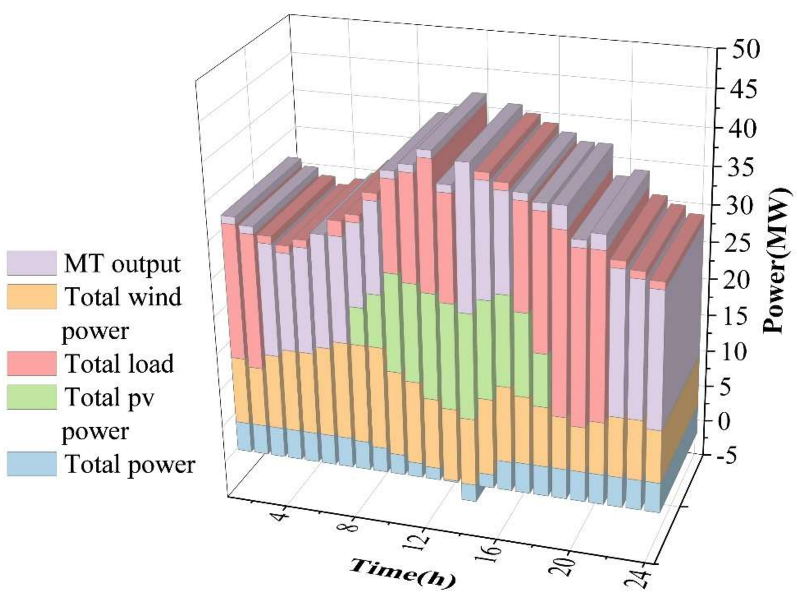

Fig. 7. The VPP is scheduled for the following date

Figure 8 shows the trend of MT output. It is the same trend as the load demand curve in Fig. 6, which is because the MT generation is to supply the load demand, so it responds to the load demand situation. In addition, the significant increase in MT output before 7:30 and after 19:30 o'clock is due to the fact that there is no PV generation during this time, and MT generation is needed to keep the balance between supply and demand. The MT output is lowest at 8:30 and 10:30, which is due to high wind and light output and relatively low load demand. At 14:30, there was a sudden increase in load demand and no significant fluctuation in scenery output, so there was a large localized rise in MT. In summary, the output result curve reflects the relationship between MT generation and load demand, and the output of MT and wind power and photovoltaic power are complementary, which indicates that the dispatch result is correct and reasonable, and proves the validity of the established model.

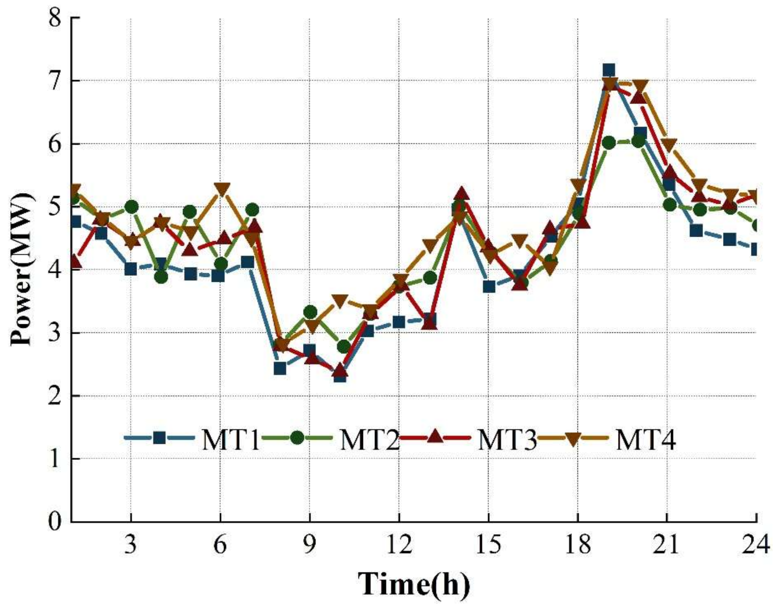

Fig. 8. MT output curve

Figure 9 shows the VPP interacting with the market power. In this case, a positive VPP power interaction with the large grid indicates that the VPP buys power from the grid; a negative VPP power interaction with the large grid indicates that the VPP sells power to the grid. Combined with the electricity price before the day in Table 5, it can be seen that since the electricity price is very low before 9:30 and after 16:30, the purchase price is lower than the cost of VPP power generation, so the VPP purchases power from the grid, thus reducing the generation of power from the generating units and lowering the cost of power generation in the system. Beginning at 9:30 a.m., the market price of electricity begins to rise, power purchases begin to fall, and VPP purchases a small amount of power from the grid to compensate for generation. Between 11 and 16 o'clock, the market price of electricity is high, higher than the cost of VPP's generation, so VPP sells electricity to the grid for revenue. The analysis shows that the purchase and sale of electricity between VPP and the grid is in line with the market law, which proves the validity and economy of the model.

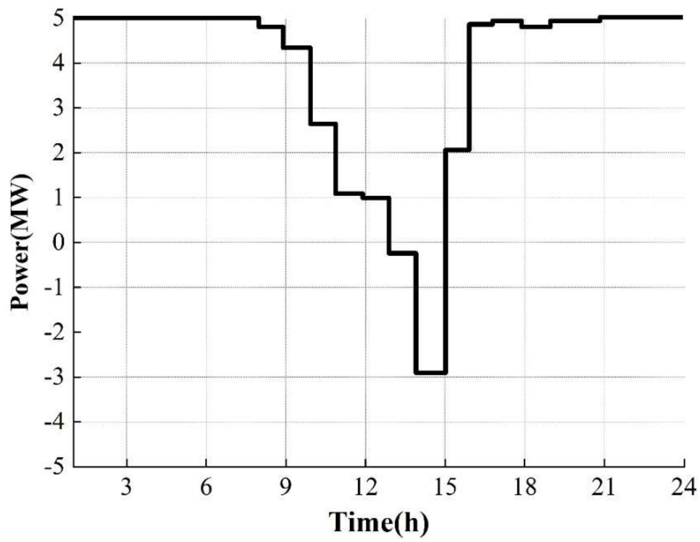

Fig. 9. VPP interacts with the main network

4. Conclusion

In this paper, in order to realize the collaborative operation of virtual power plant system and the fine management of supply and demand, a virtual power plant operation system based on complex network is designed and simulation experiments and application tests are carried out, and the following conclusions are drawn:

1) The average path of the network calculated by using the electrical distance between network nodes instead of the shortest path when analyzing the network is shorter, and the transmission energy efficiency is higher. Therefore, calculating transmission energy efficiency based on electrical distance is more realistic.

2) It can be observed that the location of the interface has a huge impact on energy efficiency regardless of whether the line is weighted or not. Therefore, the location of the system in this paper is particularly important when accessing the distribution network.

3) The average path fluctuations at the time of entitlement are roughly the same, but the system of this paper is slightly smaller compared to that of the microgrid, so the transmission is smoother and more energy efficient when the system of this paper is connected to the distribution network.

4) The MT output increases significantly before 7:30 and after 19:30, and the MT output is the least at 8:30 and 10:30. The output curves reflect the complementary output of MT, wind power and photovoltaic power, indicating that the scheduling results are correct and reasonable, and proving the effectiveness of the system established in this paper.

In conclusion, the virtual power plant operation system based on complex network designed in this paper meets the design expectation and can improve the level of virtual power plant refined management.

References

[1] Mahmud, K., Khan, B., Ravishankar, J., Ahmadi, A., & Siano, P. (2020). An internet of energy framework with distributed energy resources, prosumers and small-scale virtual power plants: An overview. Renewable and Sustainable Energy Reviews, 127, 109840.

[2] Nosratabadi, S. M., Hooshmand, R. A., & Gholipour, E. (2017). A comprehensive review on microgrid and virtual power plant concepts employed for distributed energy resources scheduling in power systems. Renewable and Sustainable Energy Reviews, 67, 341-363.

[3] Gough, M., Santos, S. F., Lotfi, M., Javadi, M. S., Osório, G. J., Ashraf, P., ... & Catalão, J. P. (2022). Operation of a technical virtual power plant considering diverse distributed energy resources. IEEE Transactions on Industry Applications, 58(2), 2547-2558.

[4] Sikorski, T., Jasiński, M., Ropuszyńska-Surma, E., Węglarz, M., Kaczorowska, D., Kostyla, P., ... & Solak, B. (2020). A case study on distributed energy resources and energy-storage systems in a virtual power plant concept: Technical aspects. Energies, 13(12), 3086.

[5] Marinescu, B., Gomis-Bellmunt, O., Dörfler, F., Schulte, H., & Sigrist, L. (2022). Dynamic virtual power plant: A new concept for grid integration of renewable energy sources. IEEE Access, 10, 104980-104995.

[6] Liu, J., Hu, H., Yu, S. S., & Trinh, H. (2023). Virtual power plant with renewable energy sources and energy storage systems for sustainable power grid-formation, control techniques and demand response. Energies, 16(9), 3705.

[7] Yang, Q., Wang, H., Wang, T., Zhang, S., Wu, X., & Wang, H. (2021). Blockchain-based decentralized energy management platform for residential distributed energy resources in a virtual power plant. Applied Energy, 294, 117026.

[8] Hu, Q., Han, R., Quan, X., Wu, Z., Tang, C., Li, W., & Wang, W. (2022). Grid-forming inverter enabled virtual power plants with inertia support capability. IEEE Transactions on Smart Grid, 13(5), 4134-4143.

[9] Aghdam, F. H., Mudiyanselage, M. W., Mohammadi-Ivatloo, B., & Marzband, M. (2023). Optimal scheduling of multi-energy type virtual energy storage system in reconfigurable distribution networks for congestion management. Applied Energy, 333, 120569.

[10] Asl, S. A. F., Bagherzadeh, L., Pirouzi, S., Norouzi, M., & Lehtonen, M. (2021). A new two-layer model for energy management in the smart distribution network containing flexi-renewable virtual power plant. Electric Power Systems Research, 194, 107085.

[11] Wang, X., Liu, Z., Zhang, H., Zhao, Y., Shi, J., & Ding, H. (2019). A review on virtual power plant concept, application and challenges. 2019 IEEE Innovative Smart Grid Technologies-Asia (ISGT Asia), 4328-4333.

[12] Bhuiyan, E. A., Hossain, M. Z., Muyeen, S. M., Fahim, S. R., Sarker, S. K., & Das, S. K. (2021). Towards next generation virtual power plant: Technology review and frameworks. Renewable and Sustainable Energy Reviews, 150, 111358.

[13] Zhang, G., Jiang, C., & Wang, X. (2019). Comprehensive review on structure and operation of virtual power plant in electrical system. IET generation, transmission & distribution, 13(2), 145-156.

[14] Adu-Kankam, K. O., & Camarinha-Matos, L. M. (2018). Towards collaborative virtual power plants: Trends and convergence. Sustainable Energy, Grids and Networks, 16, 217-230.

[15] Dall'Anese, E., Guggilam, S. S., Simonetto, A., Chen, Y. C., & Dhople, S. V. (2017). Optimal regulation of virtual power plants. IEEE transactions on power systems, 33(2), 1868-1881.

[16] Shayegan-Rad, A., Badri, A., & Zangeneh, A. (2017). Day-ahead scheduling of virtual power plant in joint energy and regulation reserve markets under uncertainties. Energy, 121, 114-125.

[17] Wang, K., Cheng, B., Ren, Y., Wang, S., Ji, R., & Kong, X. (2023). Flexible resource dynamic aggregation regulation method of virtual power plant to ensure more renewable energy generation. Process Safety and Environmental Protection, 180, 339-350.

[18] Golpîra, H., & Marinescu, B. (2024). Enhanced Frequency Regulation Scheme: An Online Paradigm for Dynamic Virtual Power Plant Integration. IEEE Transactions on Power Systems.

[19] Oshnoei, A., Kheradmandi, M., Blaabjerg, F., Hatziargyriou, N. D., Muyeen, S. M., & Anvari-Moghaddam, A. (2022). Coordinated control scheme for provision of frequency regulation service by virtual power plants. Applied Energy, 325, 119734.

[20] Esfahani, M., Alizadeh, A., Cao, B., Kamwa, I., & Xu, M. (2025). Virtual power plant formation strategy based on Stackelberg game: A three-step data-driven voltage regulation coordination scheme. Applied Energy, 377, 124355.

[21] Liu, X., Li, Y., Wang, L., Tang, J., Qiu, H., Berizzi, A., ... & Gao, C. (2024). Dynamic aggregation strategy for a virtual power plant to improve flexible regulation ability. Energy, 297, 131261.

[22] Qiu, J., Meng, K., Zheng, Y., & Dong, Z. Y. (2017). Optimal scheduling of distributed energy resources as a virtual power plant in a transactive energy framework. IET Generation, Transmission & Distribution, 11(13), 3417-3427.

[23] Yi, Z., Xu, Y., Wang, X., Gu, W., Sun, H., Wu, Q., & Wu, C. (2022). An improved two-stage deep reinforcement learning approach for regulation service disaggregation in a virtual power plant. IEEE Transactions on Smart Grid, 13(4), 2844-2858.

[24] Li, Y., Deng, Y., Wang, Y., Jiang, L., & Shahidehpour, M. (2023). Robust bidding strategy for multi-energy virtual power plant in peak-regulation ancillary service market considering uncertainties. International Journal of Electrical Power & Energy Systems, 151, 109101.

[25] Chen, S., Zhang, K., Liu, N., & Xie, Y. (2024). Unlock the aggregated flexibility of electricity-hydrogen integrated virtual power plant for peak-regulation. Applied Energy, 360, 122747.

[26] Bo Meng & Amin Rezaeipanah. (2025). Development of a multidimensional centrality metric for ranking nodes in complex networks. Chaos, Solitons and Fractals: the interdisciplinary journal of Nonlinear Science, and Nonequilibrium and Complex Phenomena115843-115843.

[27] Rachid Echarghaoui,Moussa Khouakhi & Mohamed Masmodi. (2024). The Effect of Topology on the Number of Positive Solutions for Fractional Elliptic Equations with Critical and Singular Nonlinearity. Mediterranean Journal of Mathematics(1),2-2.

[28] Piotr Narowski,Dariusz Heim & Maciej Mijakowski. (2024). New External Design Temperatures and Geospatial Models for Poland and Central Europe for Building Heat Load Calculations. Energies(16),3905-3905.